

Thermoelectric power and resistivity of $\text{HgBa}_2\text{CuO}_{4+\delta}$ over a wide doping range

Ayako Yamamoto,^{1,*} Wei-Zhi Hu,^{1,2} and Setsuko Tajima¹

¹*Superconductivity Research Laboratory, International Superconductivity Technology Center, 1-10-13 Shinonome, Koto-ku Tokyo 135-0062, Japan*

²*Tokyo University Mercantile Marine, Etchujima, Koto-ku, Tokyo 135-8533, Japan*

(Received 3 April 2000; revised manuscript received 21 July 2000; published 14 December 2000)

Thermoelectric power (TEP) and resistivity were systematically investigated for $\text{HgBa}_2\text{CuO}_{4+\delta}$ (Hg-1201) with various doping levels from high underdoping to slight overdoping. Polycrystalline Hg-1201 samples were carefully prepared from a mixture of HgO, BaO, and CuO. We paid particular attention to carbon impurity in the starting materials, resulting in a high-quality sample. This enabled us to measure reliable transport properties. Assuming one characteristic temperature T^* for each doping level, both the TEP and the resistivity can be well scaled, as was reported in the other high- T_c superconductors. The doping dependence of T^* is in good agreement with that of spin gap temperatures determined by NMR as well as that of the pseudogap temperatures reported in some other high- T_c superconductors.

DOI: 10.1103/PhysRevB.63.024504

PACS number(s): 74.72.Gr, 74.25.Fy, 74.62.Bf

I. INTRODUCTION

Recently, the pseudogap state in high- T_c superconductors (HTSC's) has been extensively studied from various experiments¹⁻³ since this state may be strongly related to the mechanism of high- T_c superconductivity. Though most properties in the pseudogap state are common in HTSC's, $(\text{La,Sr})_2\text{CuO}_4$ (La-214) shows some different behaviors from those of $\text{YBa}_2\text{Cu}_3\text{O}_{6+\delta}$ (Y-123) and $\text{Bi}_2\text{Sr}_2\text{CaCu}_2\text{O}_{8+\delta}$ (Bi-2212), for example, in the relaxation rate $(T_1T)^{-1}$ of NMR (Refs. 2 and 4) and angle-resolved photoemission spectra (ARPES).^{3,5} The origin of these differences is still an open question. One may attribute it to the number of CuO_2 layers or to the spin-charge stripe order observed clearly in La-214.⁶ In order to examine these possibilities, it is necessary to study other materials with a single CuO_2 layer per molecular formula. From this point of view, $\text{HgBa}_2\text{CuO}_{4+\delta}$ (Hg-1201) is one of the most promising candidates. Its crystal structure is simple and the superconducting critical temperature ($T_c \approx 98$ K) is the highest among the HTSC's with a single CuO_2 layer. An advantage of Hg-1201 is that the doping levels can be continuously and widely controlled from underdoping to overdoping by varying the extra oxygen content without any cation substitution.⁷

Influences of the pseudogap state can also be seen in the temperature dependence of transport properties, for example, such as the resistivity,⁸ Hall coefficient,⁹ and thermoelectric power (TEP).¹⁰ An interesting point is that these quantities in various doping levels can be scaled in a universal curve on the basis of the characteristic temperature T^* at which the temperature dependence of each quantity considerably changes.^{9,11,12} The doping dependence of T^* roughly coincides with that of the pseudogap determined from $(T_1T)^{-1}$ in NMR.² Although the scaling was successful in the in-plane data for single crystals or oriented films,¹¹ it may be applicable to high-quality polycrystalline samples if conductivity in the out-of-plane direction is negligibly small.

So far, transport properties of Hg-1201 have been reported merely as a characterization of samples. Most of the reported resistivities were rather high and the doping range

was limited.¹³ The observed high resistivity probably resulted from some undesirable intergrain impurities, which can be produced by a relatively low sintering temperature. Moreover, the superconducting transition examined by the magnetization was significantly broad, especially in the high underdoping and overdoping regions. A broad superconducting transition may be due to defects (or nonstoichiometry of cation) and/or oxygen inhomogeneity. In order to obtain reliable resistivity data, improvement on the grain surface is extremely important. In this work, we were successful in preparing good samples that exhibit a sharp superconducting transition and are appropriate for transport studies.¹⁴ By using these high-quality Hg-1201 samples, we systematically investigated the temperature dependence of their TEP and resistivity. It was found that both the TEP and the resistivity can be scaled at a characteristic temperature T^* . The doping dependence of T_c and T^* in Hg-1201 is also discussed.

II. EXPERIMENT

The Hg-1201 sample was prepared from mixtures of HgO, BaO, and CuO (99.999%) by a solid-state reaction. To minimize the carbon impurity in starting materials, the HgO powder was prepared from $\text{Hg}(\text{NO}_3)_2$ (99.999%) by heating at 350 °C for 10 h with flowing Ar (99.9999%) gas and the BaO was purified from BaCO_3 (99.997%) by sintering at 1000–1080 °C for 20 h several times under a vacuum level of about 1×10^{-3} Torr. We quantitatively analyzed the carbon content in the starting materials, because we recently found that carbon impurity is one of the important factors to control a sintering temperature^{14,15} that affects the crystallinity and the surface condition as well as the superconductivity.¹⁶ The carbon impurity determined by infrared spectroscopy LECO (CS-444LS) is 0.04, 0.15, and 0.1 at. % for HgO, CuO, and BaO, respectively. Weighing, mixing, and pelletizing of the raw materials were carried out in an Ar-filled (99.9999%, $\text{CO}_2 < 0.1$ ppm, $\text{H}_2\text{O} < 0.1$ ppm) glove box. The sample sealed in a quartz tube was sintered at 930 °C for 20 h and then quenched in cold water. It was annealed for a relatively long time (~ 1 week) to achieve

TABLE I. Structural parameters and physical properties for the nearly carbon-free $\text{HgBa}_2\text{CuO}_{4+\delta}$ samples. Hole concentration was represented by p , which was determined from the empirical relation between $S(290\text{ K})$ and p [10].

| Sample No. | Annealing conditions | a (Å) | T_c (K) | $S(290\text{ K})/\mu\text{V K}^{-1}$ | p |
|------------|-----------------------------------------|-----------|-----------|--------------------------------------|-------|
| 1 | Vac. 500 °C, 6 days | 3.8986(4) | <2 | 144 | 0.040 |
| 2 | Vac. 450 °C, 10 days | 3.8948(2) | <2 | 109 | 0.046 |
| 3 | Vac. 400 °C, 10 days | 3.8940(4) | 26 | 80 | 0.050 |
| 4 | Vac. 350 °C, 6 days | 3.8920(1) | 46 | 60 | 0.057 |
| 5 | Vac. 300 °C, 10 days | 3.8895(2) | 62 | 48 | 0.069 |
| 6 | Ar 400 °C, 10 days | 3.8869(2) | 72 | 25 | 0.090 |
| 7 | Ar 350 °C, 10 days | 3.8853(4) | 77 | 17 | 0.103 |
| 8 | Ar 300 °C, 8 days | 3.8843(4) | 83 | 9 | 0.110 |
| 9 | O ₂ 0.01% -Ar 300 °C, 7 days | 3.8825(2) | 91 | 7 | 0.119 |
| 10 | O ₂ 0.1% -Ar 300 °C, 7 days | 3.8810(3) | 95 | 6 | 0.127 |
| 11 | O ₂ 300 °C, 7 days | 3.8789(1) | 98 | 3.2 | 0.157 |
| 12 | O ₂ 240 °C, 21 days | 3.8759(3) | 92 | -0.1 | 0.180 |
| 13 | O ₂ 6 atm 320 °C, 8 days | 3.8750(3) | 86 | -3.0 | 0.190 |
| 14 | O ₂ 6 atm 270 °C, 8 days | 3.7430(4) | 80 | -4.5 | 0.208 |

oxygen homogeneity. Preliminary experiments revealed that longer annealing results in a sharp transition. We annealed samples at the different conditions for controlling oxygen contents in samples. Annealing at higher temperature with lower oxygen pressure results in a lower oxygen content, namely, a lower doping level. Annealing conditions are listed in Table I.

Impurities were not detected in the powder x-ray diffraction patterns of the as-sintered and annealed Hg-1201 samples. The neutron powder diffraction pattern of the oxygen-annealed Hg-1201 sample also indicated a single phase. A detailed crystal structure analysis will be reported elsewhere.¹⁶ The metal ratios of the as-sintered Hg-1201 sample examined by energy-dispersive x-ray analysis, using a scanning electron microscope (SEM) and inductively coupled plasma (ICP) emission spectrometry, were Hg:Ba:Cu = 1.05:1.96:1.00 and 0.95:2.00:1.00, respectively. A typical grain size of the samples observed by SEM is about $30\ \mu\text{m} \times 30\ \mu\text{m} \times 5\ \mu\text{m}$. ICP analysis revealed that there is no significant loss of Hg during the sintering and annealing processes. Oxygen contents were determined by iodometry.

The dc susceptibility χ was studied by a superconducting quantum interference device (SQUID) magnetometer under the field cooling mode with a magnetic field of 20 Oe. Measurement of the electrical resistivity was carried out by the conventional four-probe method with a current of 10 mA. Thermopower was measured using the four-probe method at temperatures from 20 to 300 K. A temperature gradient used in TEP was typically 0.3–0.5 K. Temperatures at the probe were determined using a Cu-Constantan thermocouple. The contribution from the voltage leads was carefully subtracted. In these measurements of physical properties, we paid special attention to minimize oxygen absorption at room temperature in air, especially for the highly underdoped samples. In order to avoid degradation of the sample surfaces, they were set in the apparatus for susceptibility within 5 min after

annealing and for the transport measurements within 1 h. The hole concentration (p) per a CuO_2 layer was estimated, using the Seebeck coefficient (S) at 290 K, on the basis of the empirical relation between S and p in HTSC's.¹⁰ We have confirmed that the estimated hole concentration is in good agreement with that calculated from the oxygen content.

III. RESULTS AND DISCUSSION

Figures 1(a) and 1(b) show the temperature dependence of χ for samples with various doping levels including the optimally doped sample. A doping level for each sample is indicated in Table I. In Fig. 1(a), i.e., the underdoped regime, T_c decreases as the doping level decreases, and eventually the superconductivity is not detected in sample Nos. 1 and 2. In the overdoped regime, T_c decreases with increasing doping level as shown in Fig. 1(b). Further overdoping was not successful in the present work. One possible explanation is that our samples are too dense to be oxygenated or that the oxygen diffusion rate for our less defective sample is too slow to reach equilibrium. Note that the superconducting transition is very sharp even in the highly underdoped and slightly overdoped samples, which suggests high homogeneity of the oxygen distribution in our samples. The narrow transition width ($\Delta T_c = 2\text{--}5\text{ K}$) made it possible to determine more accurately the value of T_c as well as its doping dependence. The superconducting volume fraction estimated from the ratio of the susceptibility and the Meissner signal¹⁷ is about 80% for the optimally doped sample. This large superconducting volume fraction was sustained in all samples except for heavily underdoped samples, proving that no serious deterioration was introduced by annealing. For the vacuum-annealed sample, we confirmed the recovery in superconductivity with $T_c = 97\text{ K}$ after oxygen reannealing.

Figure 2 shows the temperature dependence of the TEP for the same samples as in Fig. 1. The Seebeck coefficient (S) at 290 K for the optimally doped Hg-1201 sample (No.

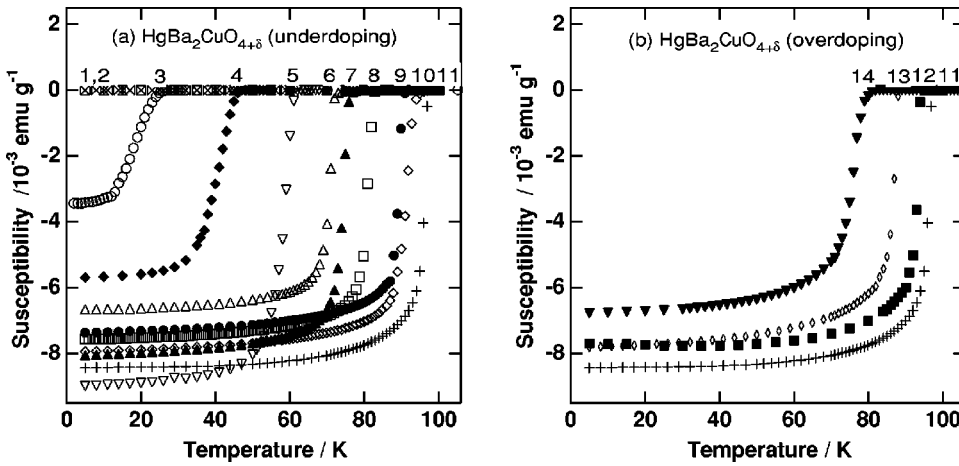


FIG. 1. dc susceptibilities of the $\text{HgBa}_2\text{CuO}_{4+\delta}$ samples annealed under various oxygen pressures and at different temperatures. (a) Underdoped and optimally doped and (b) optimally doped and overdoped. Annealing conditions are described in Table I.

11) is about $3.2 \mu\text{V/K}$, being almost comparable to $S \approx 2.3 \mu\text{V/K}$ for Bi-2212 (Ref. 12) and $S \approx 3.1 \mu\text{V/K}$ for Hg-1223.¹⁸ For the optimally doped sample, S increases with decreasing temperature with a constant slope from room temperature down to about 170 K, and has a maximum at $T \approx 130$ K, followed by a gradual decrease to zero at $T \approx 100$ K. The S at room temperature systematically decreases with doping in the underdoped regime, while in the overdoped regime, it is negative and almost linear in temperature. Such changes in $S(T)$ with doping are similar to those of the in-plane thermoelectric power for single crystals of Y-123 (Ref. 19) and Bi-2212,¹² but quite different from those of La-214.²⁰ For example, S of $\text{La}_{1.85}\text{Sr}_{0.15}\text{CuO}_4$ is $40 \mu\text{V/K}$ at 290 K, which is one order larger than the value for Hg-1201, Bi-2212, and Y-123. This suggests that the anomalous behavior of the TEP in La-214 is not related to a structural problem for a single CuO_2 layer but due to a special problem in La-214, for example, the charge ordering accompanied by a lattice distortion.⁶ Reproducibility of the

thermopower is excellent in both the absolute values and the temperature dependence.

The temperature dependence of resistivity, ρ , is shown in Figs. 3(a) and 3(b) for the same samples as those in Fig. 1. Absolute values of ρ are low for polycrystalline samples. With decreasing temperature, the ρ ($1.0 \text{ m}\Omega \text{ cm}$ at room temperature) for the optimally-doped sample (No. 11) decreases almost linearly with temperature down to about 170 K, and gradually curves downward. The zero-resistance temperature ($=96.5 \text{ K}$) is the highest value among the reported data. As doping level decreases, both the absolute value and the slope of the T -linear term in the resistivity increase. In addition, the characteristic temperature at which ρ deviates from the T -linear relation increases. These results are quite similar to the behavior of the in-plane resistivity of other HTSC's, as observed in La-214,²¹ Y-123,⁸ and Bi-2212.²² Although ρ of the overdoped sample (No. 14) exhibits a completely T -linear behavior down to T_c , its absolute value is slightly higher than that for the optimally doped sample,

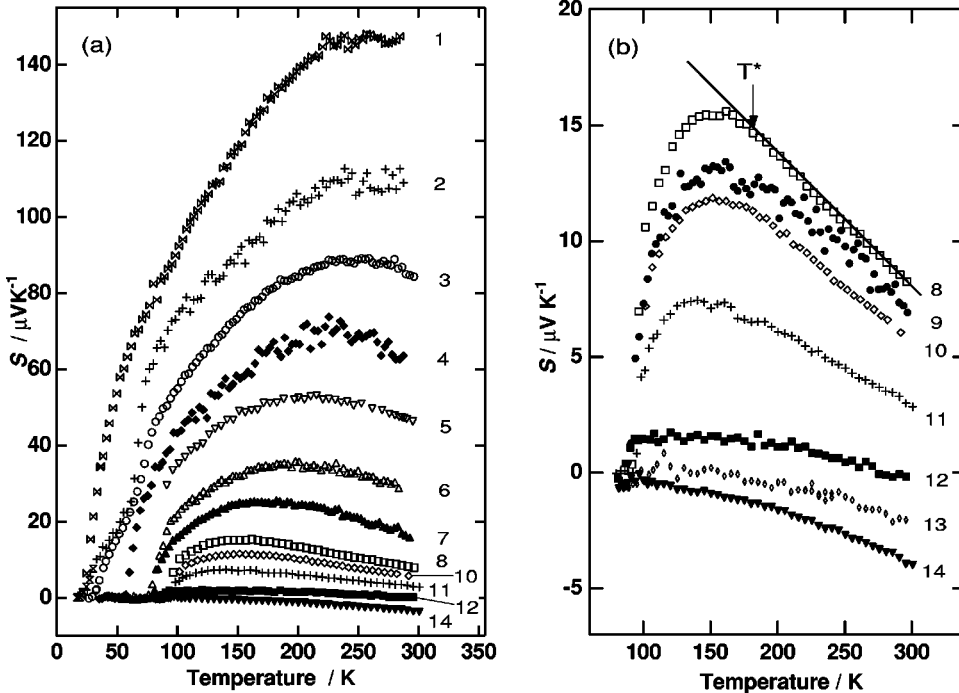


FIG. 2. Temperature dependences of thermoelectric power for $\text{HgBa}_2\text{CuO}_{4+\delta}$. (a) Over a wide doping range and (b) near the optimum doping.

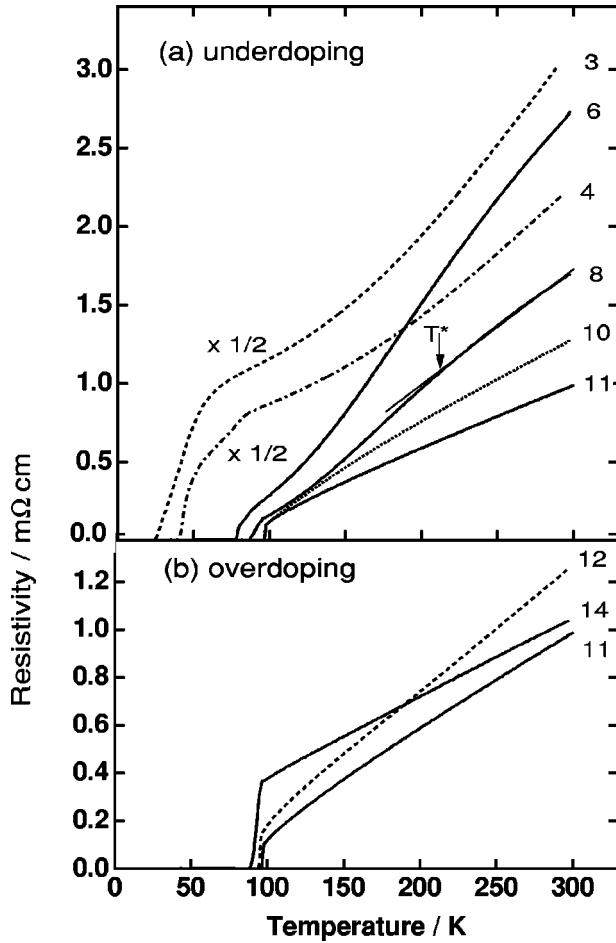


FIG. 3. Temperature dependences of resistivity for $\text{HgBa}_2\text{CuO}_{4+\delta}$ over a wide doping range. (a) Underdoped and optimally doped and (b) optimally doped and overdoped.

probably owing to some problem at the grain boundary.

These high-quality data of TEP and resistivity motivated us to examine the scaling behavior that was reported by several research groups.¹¹ Taking a certain temperature T^* that roughly corresponds to the beginning of S decrease, we normalized S by the value at T^* . Then, we obtained a beautiful scaling behavior in S for the underdoped samples, as shown in Fig. 4(a). The normalized value of S is so sensitive to the

value of T^* that the uncertainty of T^* is within 5 K. In other words, the scaling method turns out to be a good way for determination of T^* with high accuracy. Scaling analysis was also applied for the resistivity data. The universal curve was obtained as shown in Fig. 4(b). Since the effects of grain boundary on ρ cannot be completely ignored even in our high-quality samples, the uncertainty is larger than the case for $T^*(\text{TEP})$, ± 15 K, for determination of the first data point of T^* . However, once we fixed a master curve with a certain T^* , T^* for other doping levels can be determined within an accuracy of 5 K. The surprisingly well-scaled behavior of S and ρ indicates that the qualitative changes in $S(T)$ and $\rho(T)$ at T^* for various doping levels are governed by common physics, such as a change in the electronic state related to the pseudogap.

The scaling for the overdoped samples is difficult or in some cases impossible. In the case of TEP, the absolute value of S becomes close to zero when the doping level exceeds the optimum, which makes the S/N ratio worse. Moreover, the T range for scaling becomes narrow when T^* decreases, which also makes the scaling difficult. The scaling for negative values of S in the sample Nos. 13 and 14 is meaningless. As to resistivity, the scaling was not examined for the three overdoped samples (Nos. 12–14), because the effect of the grain boundary is visible in Fig. 3(b).

Another problem of the scaling would appear in the highly doped region, where the superconducting fluctuation may overcome the pseudogap effects. Since we did not distinguish the pseudogap and the fluctuation effects in our analysis, the estimated T^* might be higher than the correct values for the optimum and some highly doped samples. On the other hand, there are some theoretical models in which the pseudogap is attributed to a precursor of superconducting pairing.²³ In this case it is not necessary to distinguish the fluctuation effect from the pseudogap effect.

The doping dependence of T_c and T^* is plotted in Fig. 5. The bell-shaped T_c variation with hole concentration (p) is commonly observed in many HTSC's. The boundary of non-superconducting and superconducting phases is located at $p \approx 0.05$ and the maximum T_c is observed at $p \approx 0.16$. The increase of T_c near the nonsuperconductor to superconductor transition at $p \approx 0.05$ is very sharp, which was also reported in the La-214 system.²⁴ It may be worth noting that a plateau

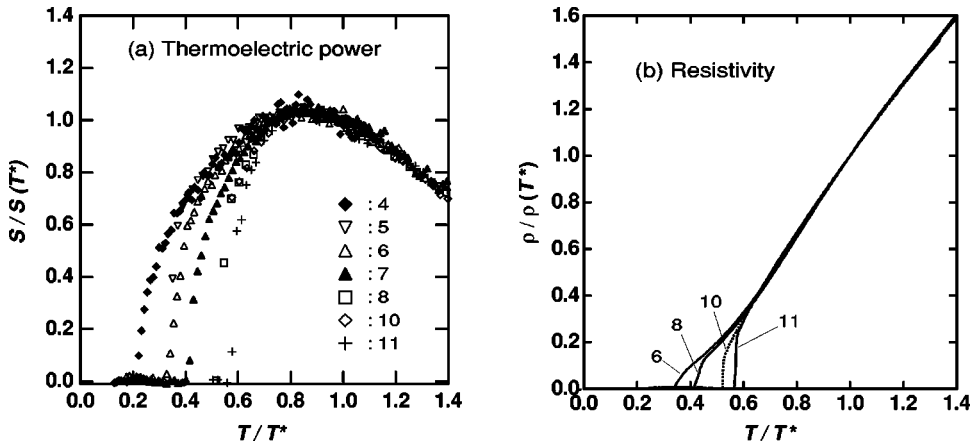


FIG. 4. Scalings of transport properties for $\text{HgBa}_2\text{CuO}_{4+\delta}$. (a) Thermoelectric power and (b) resistivity.

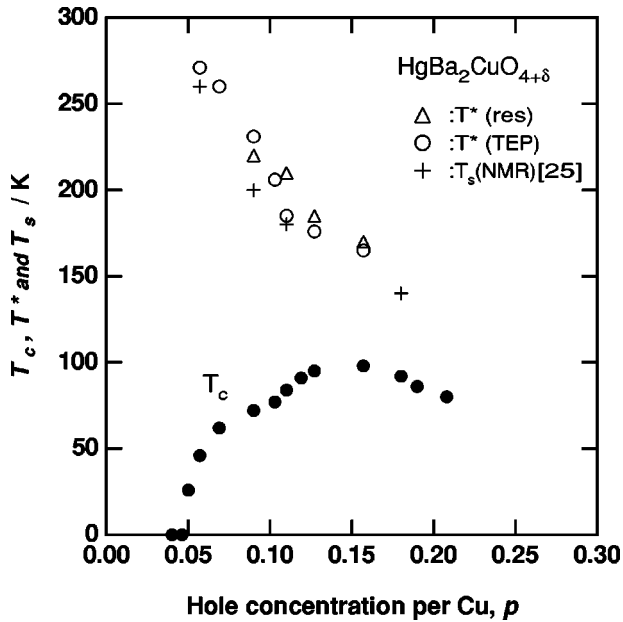


FIG. 5. The superconducting critical temperature (T_c) and the characteristic temperature (T^*) as a function of hole concentration for $\text{HgBa}_2\text{CuO}_{4+\delta}$. T_c was determined by the dc susceptibility. $T^*(\text{TEP})$ and $T^*(\text{res})$ were estimated by the temperature dependence of thermoelectric power and resistivity, respectively, as shown in Fig. 4. The spin gap temperatures determined by the NMR study are also plotted [25].

is seen at $p \approx 0.11$ which is close to the magic number of $1/8$ where a so-called stripe order was observed in La-214.⁶ To discuss it, a further careful study is required.

T^* values determined from TEP and resistivity are in good agreement, and both gradually decrease with increasing p . These temperatures are also consistent with the spin gap temperature determined by an NMR study²⁵ and are plotted together in Fig. 5. Moreover, the opening of a pseudogap in the normal state is also supported by our recent study of photoemission spectroscopy.²⁶ The obtained phase diagram in Fig. 5 is similar to that reported for other HTSC's such as Bi-2212.²⁷ A clear observation of a pseudogap in Hg-1201 excludes the possibility that a lack of clear pseudogap effects on TEP, ρ as well as NMR relaxation time in La-214, is specific to the single CuO_2 layer structure. Note that T^* is far

above T_c even at optimum doping. Although we cannot rule out the possibility that this is an artifact due to the effect of superconducting fluctuations, it is likely that this phase diagram is characteristic of the Hg-1201 system. Recently, a similar phase diagram with very high T^* has been reported for $\text{Bi}_2\text{Sr}_2\text{CuO}_{6+\delta}$ (Ref. 28) that is also a superconductor with a single CuO_2 layer in a unit cell.

IV. SUMMARY

By careful examination of carbon impurity in the starting materials and by long annealing under precisely controlled conditions, we successfully prepared Hg-1201 polycrystalline samples that are good enough for measurements of transport properties. The temperature dependence of TEP and resistivity were investigated on these high-quality Hg-1201 samples in which the doping levels were varied from being underdoped to slightly overdoped. We defined $T^*(\text{TEP})$ as the temperature at which S deviates from linearly increasing behavior and $T^*(\text{res})$ as the temperature at which $\rho(T)$ deviates from T -linear behavior. The $S(T)$ and $\rho(T)$ for various doping levels are well scaled at $T^*(\text{TEP})$ and $T^*(\text{res})$, respectively, which suggests a common origin related to the change in the electronic state. The doping dependences of $T^*(\text{TEP})$ and $T^*(\text{res})$ are almost identical, and also similar to the pseudogap behavior reported in other HTSC's. The thermoelectric power of Hg-1201 is quite different from that of $(\text{La},\text{Sr})_2\text{CuO}_4$ in spite of a similar structure with a single CuO_2 layer. The present results demonstrate that high-quality Hg-1201 can be a representative material with a single CuO_2 layer for the study of HTSC.

ACKNOWLEDGMENTS

The authors thank I. Terasaki at Waseda University and Y. Itoh at the Superconducting Research Laboratory for useful discussions. They also appreciate K. Minami of Tokyo University of Mercantile Marine for helping in resistivity and TEP measurements, and F. Izumi and Y. Yajima at the National Institute for Research in Inorganic Materials for helping in carbon analysis. This work was supported by the New Energy and Industrial Technology Development Organization (NEDO) as Collaborative Research and Development of Fundamental Technologies for Superconductivity Applications.

*Author to whom correspondence should be addressed; Fax: 81-3-3536-5714; electronic mail: yamamoto@istec.or.jp

¹C. Manabe, M. Oda, and M. Ido, *Physica C* **235-240**, 797 (1994).

²H. Yasuoka, T. Imai, and T. Shimizu, in *Strong Correlation and Superconductivity*, edited by H. Fukuyama *et al.*, Springer Series in Solid State Sciences, Vol. 89 (Springer-Verlag, Berlin, 1989), p. 254.

³A.G. Loeser, Z.-X. Shen, D.S. Dessau, D.S. Marshall, C.H. Park, P. Fournier, and A. Kapitulnik, *Science* **273**, 325 (1996).

⁴S. Ohsugi, Y. Kitaoka, K. Ishida, and K. Asayama, *J. Phys. Soc. Jpn.* **60**, 2351 (1991).

⁵A. Ino, T. Mizokawa, K. Kobayashi, A. Fujimori, T. Sasagawa, T. Kimura, K. Kishio, K. Tamasaku, H. Eisaki, and S. Uchida,

Phys. Rev. Lett. **81**, 2124 (1998).

⁶J.M. Tranqada, J.D. Axe, N. Ichikawa, A.R. Moodenburgh, Y. Nakamura, and S. Uchida, *Phys. Rev. Lett.* **78**, 338 (1997).

⁷M.B. Morosin, E.L. Venturini, J.E. Schirber, and P.P. Newcomer, *Physica C* **226**, 175 (1994); A. Fukuoka, A. Tokiwa-Yamamoto, M. Itoh, R. Usami, S. Adachi, H. Yamauchi, and K. Tanabe, *ibid.* **265**, 13 (1996).

⁸T. Itoh, K. Kanesaka, and S. Uchida, *Phys. Rev. Lett.* **70**, 3995 (1993).

⁹N.Y. Chen, V.C. Matijasevic, J.E. Mooij, and D. van der Marel, *Phys. Rev. B* **50**, 16 125 (1994).

¹⁰C. Bernhard and J.L. Tallon, *Phys. Rev. B* **54**, 10 201 (1996).

¹¹B. Wuyts, E. Osquiguil, M. Maenhoudt, S. Libbrecht, Z.X. Gao,

- and Y. Bruynseraede, Phys. Rev. B **51**, 6115 (1995).
- ¹²J.B. Mandal, A.N. Das, and B. Ghosh, J. Phys.: Condens. Matter **8**, 3047 (1996); T. Takemura, T. Kitamura, T. Sugaya, and T. Terasaki, *ibid.* **12**, 6199 (2000).
- ¹³C.K. Subramaniam, M. Paranthaman, and A.B. Kaiser, Physica C **222**, 47 (1994).
- ¹⁴A. Yamamoto, W.-Z. Hu, F. Izumi, and S. Tajima, J. Low Temp. Phys. **117**, 789 (1999).
- ¹⁵A. Yamamoto, W.-Z. Hu, F. Izumi, and S. Tajima, Physica C **335**, 268 (2000).
- ¹⁶A. Yamamoto, W.-Z. Hu, F. Izumi, and S. Tajima, Physica C (to be published).
- ¹⁷K. Kitazawa, T. Matsushita, O. Nakamura, Y. Temioka, N. Motnhira, T. Tamura, T. Hasagawa, K. Kishio, I. Tanaka, and H. Kojima, in *Proceedings of the International Conference on Superconductivity*, edited by S.K. Joshi (World Scientific Singapore, 1990), p. 241.
- ¹⁸A. Fukuoka, A. Tokiwa-Yamamoto, M. Itoh, R. Usami, S. Adachi, and K. Tanabe, Phys. Rev. B **55**, 6612 (1997).
- ¹⁹S.D. Obertelli, J.R. Cooper, and J.L. Tallon, Phys. Rev. B **46**, 14 928 (1992) .
- ²⁰J.-S. Zhou and J.B. Goodenough, Phys. Rev. B **51**, 3104 (1995).
- ²¹H.Y. Hwang, B. Batlogg, H. Takagi, H.L. Kao, J. Kwo, R.J. Cava, J.J. Krajewski, and W.F. Peck, Jr., Phys. Rev. Lett. **72**, 2636 (1994).
- ²²T. Watanabe, T. Fujii, and A. Matsuda, Phys. Rev. Lett. **79**, 2113 (1997).
- ²³V.J. Emery and S.A. Kielson, Nature (London) **374**, 434 (1995).
- ²⁴H. Sato, A. Tsukada, M. Naito, and A. Matsuda, Phys. Rev. B **61**, 12 447 (2000).
- ²⁵Y. Itoh, T. Machi, A. Fukuoka, K. Tanabe, and H. Yasuoka, J. Phys. Soc. Jpn. **65**, 3751 (1996).
- ²⁶Y. Uchiyama, W.-Z. Hu, A. Yamamoto, S. Tajima, K. Saiki, and K. Koma, Phys. Rev. B **62**, 615 (2000).
- ²⁷M. Ido, N. Momono, and M. Oda, J. Low Temp. Phys. **117**, 329 (1999).
- ²⁸M. Kugler and O. Fischer (private communication).